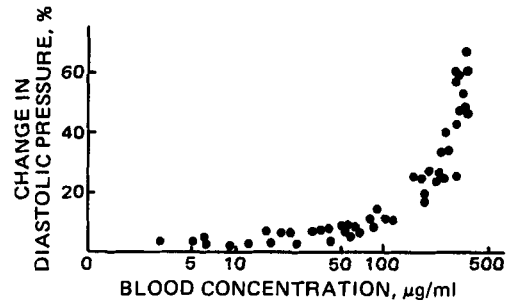

Figure 5—*Composite plot of the percent change in diastolic pressure versus the logarithm of blood concentrations of trichloromonofluoromethane in three dogs following inhalation of various strengths of the fluorocarbon in air.*

nounced. Most dogs showed biphasic responses, with an increase in the heart rate at lower doses and a decrease at higher doses (Table I). The effect on the heart rate in some dogs appeared to be instantaneous and reached a maximum within the 1st min during the inhalation in spite of the fact that the blood level continued to rise in the next few minutes.

The mechanism for such an effect is probably very complex and could not be rationalized by the multicompartmental model proposed for this fluorocarbon in dogs (14). The apparent "instantaneous" effect on the heart rate and the direct correlation between the blood level and the effect on the blood pressure and respiration rate could shed some light on the fast action of the fluorocarbon aerosol propellants, which have caused sudden death of individuals shortly after or during inhalation of large quantities of these propellants (2).

REFERENCES

(1) A. Silverglade, *J. Am. Med. Assoc.*, **222**, 827 (1972).
(2) W. S. Harris, *ibid.*, **223**, 1508 (1973).
(3) D. M. Aviado and M. A. Beles, *Toxicology*, **2**, 31 (1971).
(4) C. T. Dollery, W. M. Faith, G. H. Draffan, G. Wise, H. Sahgoun, J. W. Peterson, and S. R. Walker, *Clin. Pharmacol. Ther.*, **15**, 59 (1974).
(5) G. Marier, H. MacFarland, G. S. Wilberg, H. Buchwald, and P. Dussault, *Can. Med. Assoc. J.*, **111**, 39 (1974).
(6) E. B. Thompson and W. S. Harris, *Toxicol. Appl. Pharmacol.*, **29**, 242 (1974).
(7) W. L. Chiou, *J. Am. Med. Assoc.*, **227**, 658 (1974).
(8) *Ibid.*, **229**, 1722 (1974).
(9) D. B. Lund, *Arch. Biochem. Biophys.*, **129**, 181 (1969).
(10) P. J. Cox, L. J. King, and D. V. Parke, *Biochem. J.*, **130**, 87p (1972).
(11) H. C. Warmkier, O. Fennema, and E. H. Marth, *J. Food Sci.*, **37**, 702 (1972).
(12) V. C. Fohz and R. Fuerst, *Environ. Res.*, **7**, 275 (1974).
(13) R. J. Cicerone, R. S. Stolarski, and S. Walters, *Science*, **185**, 1165 (1974).
(14) S. Niazi and W. L. Chiou, *J. Pharm. Sci.*, **64**, 763 (1975).
(15) W. L. Chiou and S. Niazi, *Res. Commun. Chem. Pathol. Pharmacol.*, **6**, 481 (1973).
(16) J. Adir, D. A. Blake, and G. M. Mergner, *J. Clin. Pharmacol.*, **15**, 760 (1975).
(17) A. Azar, H. J. Trochimowicz, J. B. Terrill, and L. S. Mullin, *Am. Hyg. Assoc. J.*, **34**, 102 (1973).
(18) K. Chang and W. L. Chiou, *J. Pharm. Sci.*, **65**, 53 (1976).
(19) M. Gibaldi and D. Perrier, "Pharmacokinetics," Dekker, New York, N.Y., 1975.
(20) R. H. Reuning, R. A. Sams, and R. E. Notari, *J. Clin. Pharmacol.*, **13**, 127 (1973).
(21) G. Levy and R. Koysook, *J. Pediatr.*, **86**, 789 (1975).
(22) J. A. Simaan and D. M. Avaido, *Toxicology*, **5**, 127 (1975).

ACKNOWLEDGMENTS

Supported in part by Grant PHS-FD 574-03 from the Food and Drug Administration.
The assistance of Mr. Djebra Kasabdji is gratefully acknowledged.

Solution Rate of Crystals at Fluid–Fluid Interface

A. J. M. SCHOONEN ˣ, G. W. de VRIES-NIJBOER, and T. HUIZINGA

Received December 27, 1977, from the *Department of Pharmaceutics, Subfaculty of Pharmacy, University of Groningen, Anthonius Deusinglaan 2, Groningen, The Netherlands.* Accepted for publication June 30, 1978.

Abstract □ A model system was developed in which the dissolution behavior of a single crystal of potassium ferricyanide was studied at a liquid paraffin–water interface. Since the equilibrium position of a crystal at the interface is independent of its size, the lifetime of a crystal dissolving at the interface is determined entirely by its initial size and its dissolution rate in the water phase. The dimensions of every crystal were measured microscopically before dissolution. A continuous-flow recording dissolution apparatus was used to measure spectrophotometrically the mass flow of dissolved potassium ferricyanide. The dissolution cell in this system was mounted in an optical bench, making it possible to follow dissolving crystals visually by projecting them on a screen. The results show that the lifetime of a crystal is proportional to the shortest length of the crystal face in contact with the liquid paraffin and is rather independent of its form. Furthermore, crystal shape changes during dissolution, which is explained partly by the nonisometric dissolution of potassium ferricyanide crystal faces and partly by the nonconstancy of film thickness.

Keyphrases □ Dissolution—potassium ferricyanide crystals at fluid-fluid interface □ Potassium ferricyanide—dissolution of crystals at fluid-fluid interface □ Crystal dissolution—potassium ferricyanide at fluid-fluid interface

The lifetime of a solid particle dissolving in a liquid is governed by its rate of change in surface area. Assuming a constant hydrodynamic boundary layer, Hixson and Crowell (1) derived the cube root law for the dissolution of sodium chloride crystals:

$$w_0^{1/3} - w_t^{1/3} = Kt \qquad \text{(Eq. 1)}$$

where w_0 is the weight of the particle at $t = 0$, w_t is the weight of the particle at time t, and K is a dissolution rate constant also composed of density and a shape factor. Many deviations from the cube root law were found, but it was difficult to explain the results because of the experimental design (in which often a number of particles were employed in a stirred system). In the experiments of Niebergall *et al.* (2) and Hixson and Crowell (3), the rate constant increased as dissolution proceeded. A linear re-

0022-3549/79/0200-0163$01.00/0

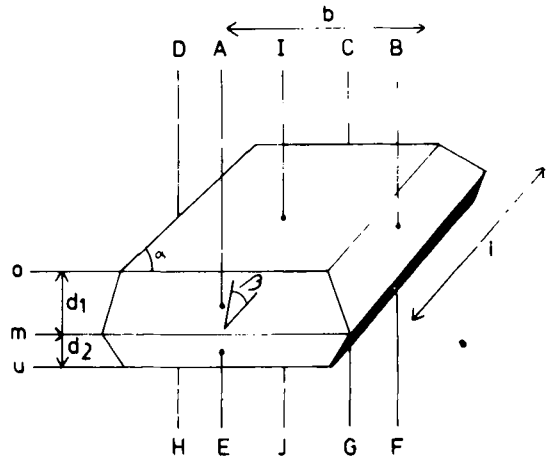

Figure 1—*Shape of a potassium ferricyanide crystal.*

lationship between the film thickness and the square root of particle weight was postulated (2), assuming a constant shape factor, which gives:

$$w_0^{1/2} - w_t^{1/2} = Kt \qquad \text{(Eq. 2)}$$

Wilhelm *et al.* (4), working with crystals of sodium chloride, reported the opposite effect: a decreasing rate during dissolution.

McCabe and Stevens (5) investigated crystal growth of copper sulfate and found a decrease in the growth rate for smaller particles in a stirred system; under conditions of constant shear, however, the growth rate was constant. The influence of the shape factor was recognized, and conditions were chosen such that it was practically constant (5).

Veng Pedersen and Brown (6, 7) developed equations for nonspherical particles, assuming a constant dissolution rate. By using a spherical approximation, they examined a 60–85-mesh fraction of tolbutamide in a system under conditions of constant shear. In spite of the fact that a changing shape factor was taken into account, it was difficult to discriminate between Eqs. 1 and 2 as the best fit for the experimental data.

Clearly, particle dissolution is still not very well explained. In the present study, single crystals of potassium ferricyanide were investigated by employing a dissolution cell in which the crystals dissolve at a liquid paraffin–water interface, enabling simultaneous measurement of the mass flow and particle size.

THEORETICAL

The simplest case of particle dissolution is that of an isometrically shaped crystal (length = width = height) that is dissolving isotropically; *i.e.*, each point on each crystal face is retreating at the same rate.

For a cube with a linear diameter, b, it can be written:

$$-\frac{db}{dt} = 2\sigma \qquad \text{(Eq. 3)}$$

where σ is the retreat rate of one crystal face.

Equation 3 integrates to:

$$b_0 - b_t = 2\sigma t \qquad \text{(Eq. 4)}$$

where b_0 is the dimension at $t = 0$ and b_t is the dimension at time t.

If each crystal face is retreating at the same rate at any time t, a cube is dissolving isometrically; *i.e.*, there is a constant relationship between b, the surface, S, and the volume or weight, W, of the cube throughout the dissolution process:

$$b_t = (\tfrac{1}{6} S_t)^{1/2} = (W/\rho)^{1/3} \qquad \text{(Eq. 5)}$$

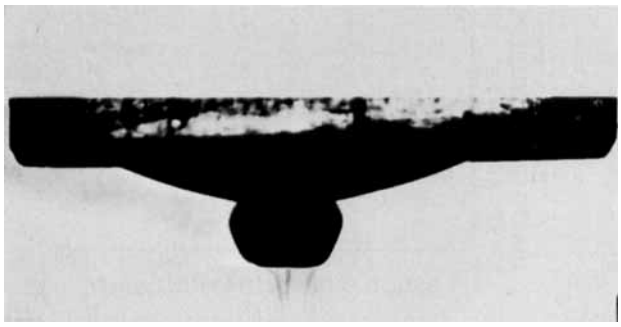

Figure 2—*Photograph of the projection of a potassium ferricyanide crystal in the equilibrium position at a liquid paraffin–water interface.*

where ρ is density. Substitution of Eq. 5 in Eq. 4 yields the cube root law (Eq. 1) or its equivalent:

$$S_0^{1/2} - S_t^{1/2} = 2\sqrt{6}\sigma t \qquad \text{(Eq. 6)}$$

According to Eq. 6, a plot of $S_t^{1/2}$ *versus* time should be a straight line when the cube root law is valid.

Since the mass flow, Q_t, at time t is proportional to the surface at that time for every heterogeneous reaction, it can be written:

$$Q_t = \rho\sigma_t S_t \qquad \text{(Eq. 7)}$$

where σ_t is the retreat rate at time t. Therefore, a plot of $Q_t^{1/2}$ *versus* time also yields a straight line when the cube root law is valid.

Dissolution at an Interface—At an interface, the simplest case of particle dissolution is that for half a cube ($b \times b \times \frac{1}{2}b$) dissolving isotropically. With the assumption that only one face of the cube ($b \times b$) is in contact with the upper fluid and does not take part in the dissolution process, the surface area exposed to the solvent phase is, at any time t:

$$S_t = 4(b_t \tfrac{1}{2} b_t) + b_t^2 = 3b_t^2 \qquad \text{(Eq. 8)}$$

Substitution of Eq. 8 in Eq. 4 gives:

$$S_0^{1/2} - S_t^{1/2} = 2\sqrt{3}\sigma t \qquad \text{(Eq. 9)}$$

Therefore, when half a cube dissolves isotropically at an interface, a plot of $S_t^{1/2}$ or $Q_t^{1/2}$ *versus* time also is linear.

Although Eq. 2 assumes an increasing dissolution rate, at any time t the rate is equal for each crystal face, which means that Eq. 5 is valid in this case. Therefore, substitution of Eq. 5 in Eq. 2 yields:

$$S_0^{3/4} - S_t^{3/4} = Kt \qquad \text{(Eq. 10)}$$

The mass flow, Q_t, at any time t for half a cube at an interface is obtained with Eqs. 4, 7, and 8:

$$Q_t = 3\rho\sigma(b_0 - 2\sigma t)^2 \qquad \text{(Eq. 11)}$$

where σ is a constant if Eq. 1 is valid and $\sigma = f(1/b)^{1/2}$ if Eq. 2 is valid.

Dissolution of a Crystal of Potassium Ferricyanide—The shape

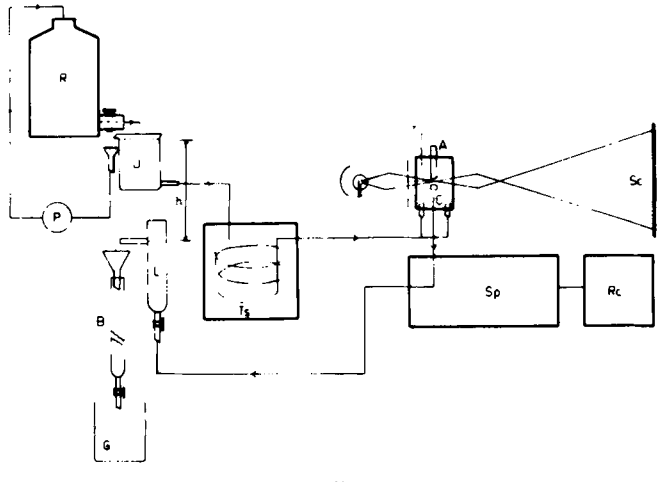

Figure 3—*Continuous-flow recording apparatus.*

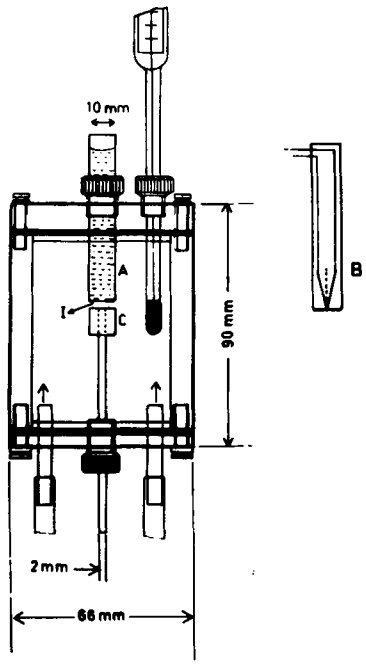

Figure 4—*Dissolution cell. Tube A contains liquid paraffin, forming an interface at I. For calibration, tube B is inserted instead of tube A and is connected with a microburet.*

of a potassium ferricyanide crystal with surfaces S_A, S_B, S_C, *etc.*, is shown in Fig. 1. If crystal face I is in contact with the upper fluid at a fluid–fluid interface, the total area, S, in contact with the solvent is given by:

$$S = S_J + (S_E + S_F + S_G + S_H) + (S_A + S_B + S_C + S_D) \quad \text{(Eq. 12)}$$

Assume that Eq. 4 is valid for some points on the "vertical" faces (A–I). The parameter σ is defined as the rate of retreat directed parallel to the interface and in a plane perpendicular to the retreating crystal face. In this way, σ has the same direction as it would have if the crystal were half a cube. Also assume that a point on the "horizontal" face J is retreating according to Eq. 4 but at a different rate τ.

To eliminate "rounding off" effects at the edges of the crystal faces and a different thickness of the hydrodynamic boundary layer for one face, it is necessary to assume that all points on a certain face are retreating with the same velocity: σ for faces A–I and τ for face J. Since $S_E = S_G$, $S_F = S_H$, $S_A = S_C$, $S_B = S_D$, and α is assumed to equal 90°, the mass flow of a potassium ferricyanide crystal at time t is given by:

$$Q_t = \rho[(S_J)_t\tau + (2S_E + 2S_F)_t\,\sigma \sin\beta + (2S_A + 2S_B)_t\sigma \sin\beta] \quad \text{(Eq. 13)}$$

Crystal faces A–I are trapezoids, whose areas may be expressed in linear dimensions:

$$(S_A)_t = \tfrac{1}{2}(b_{0_t} + b_{m_t})d_{1_t}/\sin\beta \quad \text{(Eq. 14)}$$

$$(S_B)_t = \tfrac{1}{2}(l_{0_t} + l_{m_t})d_{1_t}/\sin\beta \quad \text{(Eq. 15)}$$

$$(S_E)_t = \tfrac{1}{2}(b_{u_t} + b_{m_t})d_{2_t}/\sin\beta \quad \text{(Eq. 16)}$$

$$(S_F)_t = \tfrac{1}{2}(l_{u_t} + l_{m_t})d_{2_t}/\sin\beta \quad \text{(Eq. 17)}$$

Crystal face J may be expressed as:

$$(S_J)_t = (b_{u_t})(l_{u_t}) \quad \text{(Eq. 18)}$$

Due to the shape of a potassium ferricyanide crystal, the retreat rate for dimensions b_u and l_u is also influenced by the rate of decrease of d_2; so for b_{u_t}:

$$(b_{m_t} - b_{u_t})/(b_m - b_u) = d_{2_t}/d_2 \quad \text{(Eq. 19)}$$

With the aid of Eq. 4, it can be written:

$$b_{u_t} = b_u - 2\sigma t + \tau t(b_m - b_u)/d_2 \quad \text{(Eq. 20)}$$

Also:

$$l_{u_t} = l_u - 2\sigma t + \tau t(l_m - l_u)/d_2 \quad \text{(Eq. 21)}$$

By substituting Eq. 4 for the dimensions b_{m_t}, b_{0_t}, l_{m_t}, and l_{0_t} and the relation for b_{u_t} and l_{u_t} in Eqs. 14–18, expressions are obtained in which the area of the crystal in contact with the solvent phase can be calculated at any time t, if σ, τ, and the initial dimensions of the crystal are known.

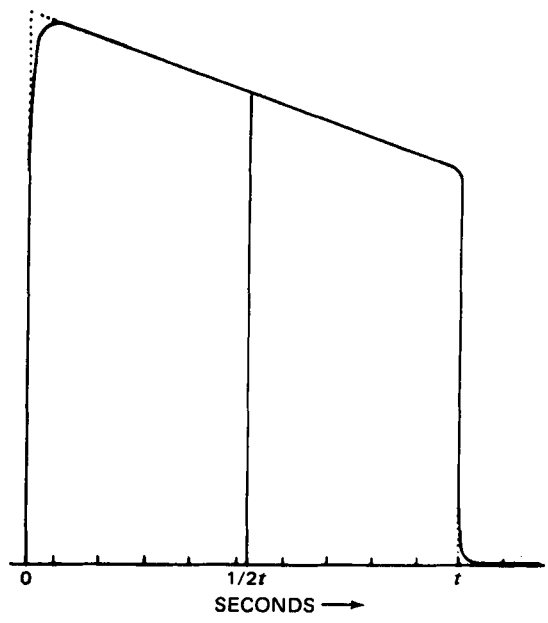

Figure 5—*Calibration curve.*

Finally, the following equation is obtained for the mass flow at time t by substitution of Eqs. 14–19 in Eq. 13:

$$Q_t = \rho\{[l_u - 2\sigma t + \tau t(l_m - l_u)/d_2][b_u - 2\sigma t + \tau t(b_m - b_u)/d_2]\tau + [b_u + \tau t(b_m - b_u)/d_2 + b_m + l_u + \tau t(l_m - l_u)/d_2 + l_m - 8t\sigma] \times (d_2 - \tau t)\sigma + [b_0 + b_m + l_0 + l_m - 8\sigma t]d,\sigma\} \quad \text{(Eq. 22)}$$

Equation 22 can be used to describe the dissolution of a potassium ferricyanide crystal until $d_2 = 0$ or $b_u = 0$. If a potassium ferricyanide crystal can be idealized to half a cube with a rate of decrease of σ for the vertical faces and τ for the horizontal face, Eq. 22 simplifies to:

$$Q_t = \rho[4\sigma(\tfrac{1}{2}b - \tau t)(b - 2\sigma t) + (b - 2\sigma t)^2\tau] \quad \text{(Eq. 23)}$$

EXPERIMENTAL

Crystals of potassium ferricyanide were obtained by recrystallization in an isothermal fashion from distilled water. The fluid–fluid system was liquid paraffin and distilled water. A single crystal was allowed to fall through the upper fluid. When it approached the lower fluid, distilled water, it was oriented by the interface in such a way that crystal face I or J (Fig. 1) was usually the lower face that was wetted first.

It is advantageous to use the notation described in Fig. 1, with the interface as a plane of reference. Therefore, face I is defined now as the upper crystal face.

During the wetting process, one of two things can happen. If the crystal has a size greater than its "critical size" ($b_0 > 2.5$ mm in this system), it is wetted completely and falls away from the interface. If the crystal is smaller than its critical size, it takes up an equilibrium position at the interface as is shown in Fig. 2. Since the edges of the upper crystal face I present a barrier in the wetting process, the equilibrium position is independent of particle size. Therefore, the area of surface in contact with the solvent is known accurately and can be calculated readily.

Apparatus—Figure 3 shows the continuous flow recording system. Reservoir R, together with pump P, maintains a constant height of dissolution liquid, distilled water, in vessel U. The liquid passes through thermostat Ts, which adjusts the liquid temperature when it reaches the dissolution cell. This cell is mounted in an optical bench, which makes it possible to project the dissolving crystal on screen Sc.

Liquid from the dissolution cell passes through a flowcell[1] in spectrophotometer[2] Sp, fitted with a chart recorder[3], and maintains a constant height of liquid in vessel L. The difference in height, h, between vessels

[1] Hellema; 80 μl.
[2] Beckman model DB-GT.
[3] Servogor.

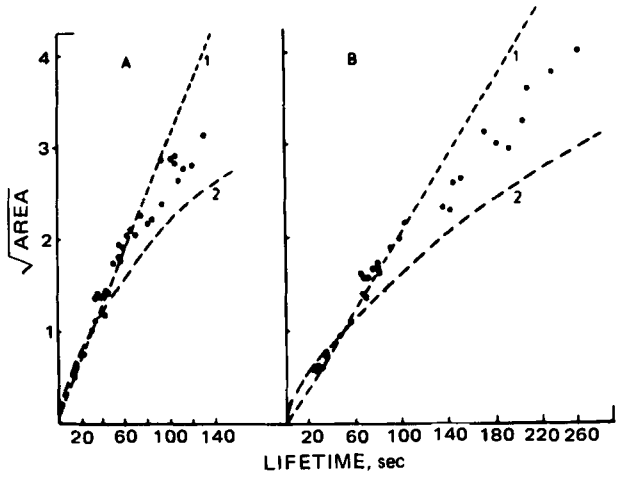

Figure 6—*Lifetime of crystals* versus *square root of area to the water phase. Each symbol represents a crystal. Key: A, streamline flow (slit width of 1.6 mm); B, free convection (slit width of 8 mm); curve 1, theoretical curve if Eq. 1 is valid; and curve 2, theoretical curve if Eq. 2 is valid. For reasons of comparison, this last curve was transformed to an (area)$^{1/2}$ axis and should be linear in an (area)$^{3/4}$* versus T *plot.*

U and L causes a pressure difference that governs the flow rate and keeps the column of liquid paraffin A in place. The interface is a sensitive detector itself for pressure differences that may develop during an experiment. The water flow is measured in buret B and finally accumulates in collection vessel G.

The dissolution cell (Fig. 4) is made of methacrylate polymer[4] and is filled with distilled water entering *via* four stainless steel tubes in every corner of the bottom to minimize turbulency. The solvent leaves the cell *via* tube C, which has a small inner diameter (2 mm), so that the solvent is transported rapidly to the spectrophotometer.

The distance between interface I and tube C (slit width) was 1.6 mm for the experiments in which the lifetime of a crystal was measured at different flow rates. The slit width was 8 mm for the experiments in which the mass flow was measured for the free convection case. At this distance, the influence of the solvent flow used (1 ml/sec) on the dissolution rate of the crystals at the interface was negligible, as was easily checked by comparing the dissolution rates obtained under these conditions and those obtained with zero solvent velocity.

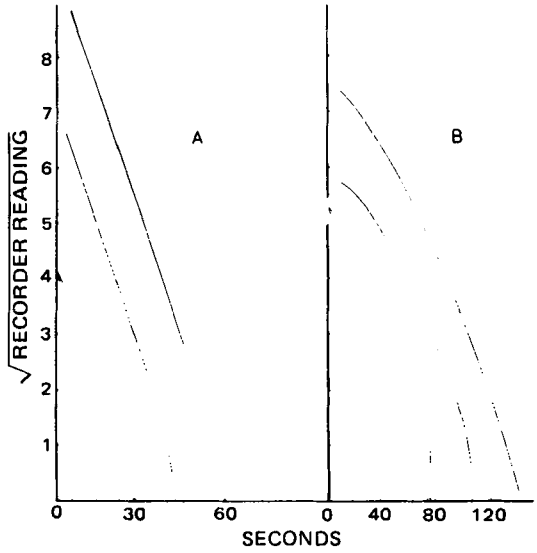

Figure 7—*Dissolution of single crystals of potassium ferricyanide. If the cube root law is valid, a straight line (broken line) should be obtained in this plot. Recorder reading = constant × mass flow at time t measured spectrophotometrically. Key: A, streamline flow (slit width of 1.6 mm); and B, free convection (slit width of 8 mm).*

[4] Perspex.

Table I—Mean Values of Height ($\bar{d}$), Length ($\bar{l}$), and Width ($\bar{b}$) for Crystals of Potassium Ferricyanide Measured Individually[a]

Size Group $(\bar{l} \times \bar{b})^{1/2}$, mm	$\bar{d}$, mm	$\bar{l}$, mm	$\bar{b}$, mm	Shape Factor, $j = (\bar{l} \times \bar{b} \times \bar{d})^{1/3}/\bar{b}$
0.20–0.39	0.18	0.35	0.30	0.888
0.39–0.59	0.23	0.49	0.42	0.861
0.59–0.78	0.25	0.75	0.58	0.823
0.78–0.98	0.33	1.01	0.79	0.811
0.98–1.18	0.39	1.23	0.89	0.846
1.18–1.37	0.49	1.36	1.19	0.778
1.37–1.57	0.56	1.58	1.39	0.771
1.57–1.76	0.54	1.80	1.57	0.773
1.76–1.96	0.60	1.95	1.76	0.723

[a] The mean value of a dimension of the crystal is the arithmetic mean for that dimension of all crystals in the given size group.

At the same time, the acceleration of the dissolved mass began close enough to the crystal surface to prevent differences in transportation time to tube C due to differences in density. This was checked by comparing the lifetime of a crystal as measured by eye using a stopwatch and the total dissolution time as recorded spectrophotometrically. The difference between these two values was never more than 2 sec.

The temperature in the dissolution cell was maintained at 20 ± 0.1°. Crystal sizes were measured microscopically. The projections of a crystal on the screen were photographed at regular time intervals to determine the retreat rate of some points on its circumference.

Calibration—The apparatus was calibrated with the aid of a microburet fixed at a certain height and connected with tube B, which was installed instead of tube A (Fig. 4). Before every measurement, the buret was filled with 0.03% potassium ferricyanide to the exact same height. A 5-ml volume of this solution was allowed to flow into the dissolution cell, and the time needed was measured. The density difference between this concentration and pure water is small, so convection through the orifice of tube B was negligible.

Figure 5 shows a registration of a particular measurement. The mass flow decreased linearly as the meniscus of the solution in the buret was losing height. Ideally, the registration should follow the dotted line. The deviation was caused mainly by a velocity gradient inside the hose connecting the dissolution cell with the flowcell. The value at half-time measured from the end-point at t was used as the mean scale reading. The calibration constant, F, was calculated as follows:

$$F = \frac{\text{mass flow recorded}}{\text{mass flow from buret}} = \frac{uy/a}{cv/t} \qquad \text{(Eq. 24)}$$

where u is the recorder reading, y is the solvent flow rate measured during calibration, a is the scale expansion factor, c is the concentration of potassium ferricyanide in the buret, and v is the volume of solution that has flowed out of the buret in time t.

As a check on the accuracy of the instrument, y was varied. If the mass flow from the buret is constant, u should be inversely proportional to y and F should be constant. The value of F was calculated 14 times at four

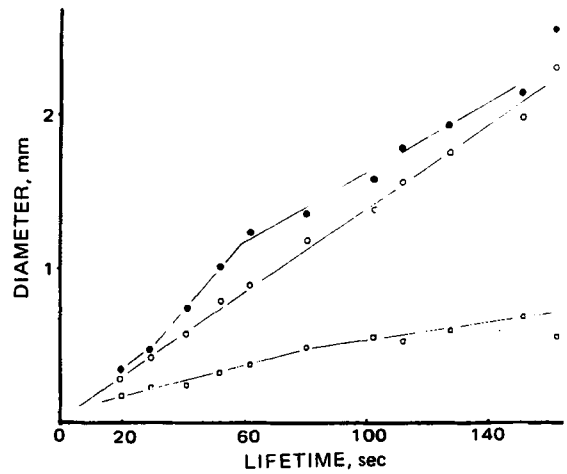

Figure 8—*Plot illustrating the relationship between the mean dimensions of crystals of potassium ferricyanide and lifetime (values from Table I). Key: ●, length; ○, width; and □, height.*

Table II—Accuracy of Measurements ($\Delta G\%$), Size Data, Dissolution Rate Constants, and Deviation in Prediction of $t = T$ by Eqs. 11 and 23 for Eight Crystals ($\Delta T\%$) [a]

Crystal	$\Delta G\%$	b_0, mm	b_{calc}, mm	d/b_0	d/l_0	σ, $\times 10^{-3}$ mm/sec	τ, $\times 10^{-3}$ mm/sec	ΔT, %
1	−1.4	0.72	0.71	0.51	0.47	5.5	2.3 → 2.3	2.-
2	+0.3	0.93	0.78	0.32	0.28	6.0	2.4 → 3.7	16.2
3	−10.2	1.15	1.13	0.60	0.50	5.6	2.7 → 6.8	1.4
4	−5.3	1.59	1.30	0.21	0.16	6.4	1.8 → 3.8	18.4
5	−5.5	0.74	0.91	0.82	0.72	4.9	3.1 → 6.7	22.8
6	+3.4	1.50	1.37	0.42	0.36	6.2	2.2 → 5.3	9.1
7	+1.3	0.98	0.73	0.34	0.32	6.6	3.1 → 3.1	25.7
8	+2.1	1.33	1.04	0.25	0.23	6.3	2.2 → 3.6	22.-

[a] The abbreviations used are: ΔG = (area under experimental curve − area under calculated curve) × 100%/(area under experimental curve) (Fig. 11), b_0 = microscopically measured width of crystal face I (Fig. 1), b_{calc} = dimension of half a cube with the same weight as the crystal: b_{calc} = (weight of crystal/0.5ρ)$^{1/3}$, d = microscopically measured height of the crystal (shortest distance between faces I and J), l_0 = microscopically measured length of crystal face I, σ = rate of retreat of "vertical" crystal faces A–I, and τ = rate of retreat of "horizontal" crystal face J.

different flow rates, ranging from 0.5 to 1 ml/sec. The variation coefficient was 1.3%.

RESULTS AND DISCUSSION

In the first series of experiments, results for single-crystal dissolution were compared with the results for monosized particles obtained by Niebergall *et al.* (2). Therefore, the dimensions of a number of crystals were measured. The length and width of the crystals were defined as the mean values of the dimensions of crystal faces I and J, respectively (Fig. 1).

A plot of the square root of the area exposed to the water phase *versus* the lifetime of the crystal is shown in Fig. 6. If the cube root law is valid, a plot of $S_0^{1/2}$ *versus* lifetime should yield a straight line according to Eq. 9. Also a plot of $S_0^{3/4}$ *versus* T (Eq. 10) is included to compare Eqs. 1 and 2. Although neither of these equations describes the dissolution process accurately, it is clear that the dissolution rate increases with decreasing particle size. The dissolution curves of individual crystals measured spectrophotometrically also show an increasing rate constant.

Figure 7 was obtained by plotting the square root of the recorder reading (= constant × mass flow) *versus* t. As shown in the *Theoretical* section (Eqs. 6 and 7), a plot of $Q_t^{1/2}$ or (recorder reading)$^{1/2}$ *versus* time should be linear if the cube root law is valid.

Although the method of measurement is different from that of Niebergall *et al.* (2), the same questions can be asked:

1. Is there a nonlinear retreat of the surface caused, for instance, by a dependency of the hydrodynamic boundary layer on particle size?
2. Is the shape factor changing because of a nonisometric shape of the crystal or because of a different hydrodynamic boundary layer for different crystal faces?

A first indication that a changing shape factor might be important can be seen in Fig. 7, where the curvature is more pronounced for the crystals dissolving under conditions of free convection (slit width of 8 mm). By visual examination of the projected crystal during dissolution, it became clear that the crystal was changing its form when a solvent flow rate of more than 0.15 ml/sec was applied with a slit width of 1.6 mm. Then the solvent entering the slit radially accelerated to a high velocity, especially attacking the edges of crystal face J if I were in contact with the liquid paraffin. The crystal rapidly changed until a pyramid formed. These differences in form could very well explain the differences in curvature.

A second indication is provided by Table I. All of the measured crystals were classified in groups, and the mean diameters were determined to obtain a shape factor for each size group. This factor changed with particle size. Since approximately the same amount of crystals was used in the same size group for every flow rate measured, it was possible to calculate a mean dissolution time for each size group.

Figure 8 is a plot of the mean diameters of the size classes *versus* the mean dissolution time. These data show that the cube root law is not valid for these crystals due to the dependency of shape on particle size and also that there is a linear relationship between the width, b, of a crystal and its lifetime. When, however, the width of individual crystals was plotted *versus* dissolution time, the results varied widely, making it impossible to explain this relationship.

One reason for this variation could be that only the width of face I or J exhibited the constant rate of decrease while the mean value of the width of both faces was measured. It was assumed that the dimensions of face I in contact with the liquid paraffin probably showed linear dissolution behavior because the circumference of that crystal face was the leading edge and, therefore, independent of the dissolution behavior of other points on the crystal surface. Moreover, the lifetime of a crystal at the interface is determined by the shortest dimension of that face; when it is zero, either the crystal is completely dissolved or it is falling from the interface. Therefore, in a new series of experiments, the actual value of b_0 was measured, as was the lifetime of the crystals at different flow rates.

Figure 9 clearly shows that the rate of decrease of b_0 is independent of particle size. The linear retreat of points on the circumference of crystal face I is affirmed by measurements on the projected diameter of that face (Fig. 10). It can be concluded, therefore, that all diameters of face I decrease with about the same rate. The shortest of these, b_0, terminates the dissolution process by forcing the other parameters to zero. For this diameter, independent of the shape of the crystal, Eq. 4 is valid.

Due to the changing shape of the crystals during dissolution, the cube root law cannot be used to calculate the mass flow of dissolved potassium

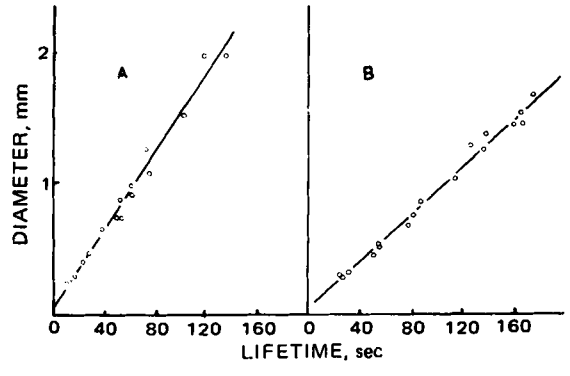

Figure 9—*Plot showing the proportionality between the width, b_0, of crystals of potassium ferricyanide and their lifetime. Key: A, streamline flow (slit width of 1.6 mm); and B, free convection (slit width of 8 mm).*

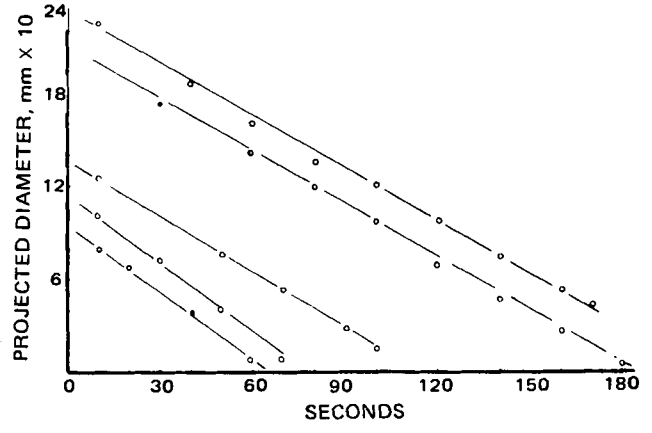

Figure 10—*Decrease of the projected width of crystal face I as a function of time. Only the shortest diameter, b_0, decreases linearly to zero; the others also decrease at about the same rate but are forced to zero at the end of the dissolution process.*

Table III—Percent Deviation of Q_t Values Predicted by Eqs. 22, 11, and 23 from the Measured Value at $t = 0.25T$, $0.5T$, and $0.75T$ for Eight Crystals from Table II [a]

Crystal	Eq. 22			Eq. 11			Eq. 23		
	$0.25T$	$0.5T$	$0.75T$	$0.25T$	$0.5T$	$0.75T$	$0.25T$	$0.5T$	$0.75T$
1	−4	−4	−3	+2	−1	−13	−3	−5	−5
2	0	−1	−2	+6	−16	−14	+3	−7	−10
3	−6	−5	−3	+9	−12	−15	+5	−5	−10
4	−5	−8	−3	+8	−19	−17	+5	−6	−12
5	−6	−6	−6	+3	−7	−10	−2	−5	−5
6	−6	−2	0	+5	−13	−12	+1	−3	−5
7	−5	−3	0	−25	−26	−15	−25	−21	−15
8	−1	−6	−2	+2	−22	−15	+1	−12	−13

[a] The percentages deviation were calculated according to the following equation: [Q_t (measured curve) − Q_t (calculated curve of Eq. 22)] × 100%/Q at $t = 0$ from the calculated curve of Eq. 22 (Fig. 11).

ferricyanide. Therefore, Eq. 22 was derived in which the mass flow, Q_t, is expressed in the linear dimensions of the crystal. Under conditions of free convection (slit width of 8 mm), crystal face J does not deform and can be identified as a separate face during the entire process. Therefore, this case was investigated further.

Numerous crystals were measured accurately; photographs were taken during dissolution, and the total dissolution time was measured. It was assumed that all crystal faces but face J were retreating linearly at a rate of σ mm/sec into a direction parallel to the interface. Crystal face J retreated with a lower velocity and in a nonlinear fashion as measured from the photographs, so these variable values for τ were used in the calculation of the dissolution curve from Eq. 22.

The weight of the crystal was calculated by comparing the area under the curve of the crystal with the area under a calibration curve for which the corresponding amount of potassium ferricyanide was exactly known. Since the area under the curve should be the same for the measured curve and the one calculated with the aid of Eq. 22, the difference in weight, ΔG (Table II), was calculated as a measure of accuracy. Then the mass flow was calculated for half a cube obeying the cube root law, which had the same weight as the crystal (Eq. 11). Here b was calculated from $b = (W/0.5\rho)^{1/3}$ (where W = weight of the crystal). Also the mass flow was calculated for half a cube in which the actual values of τ were inserted, according to Eq. 23.

The percentage deviation of the mass flow calculated according to Eqs. 11, 22, and 23 from the mass flow measured spectrophotometrically is shown in Table III.

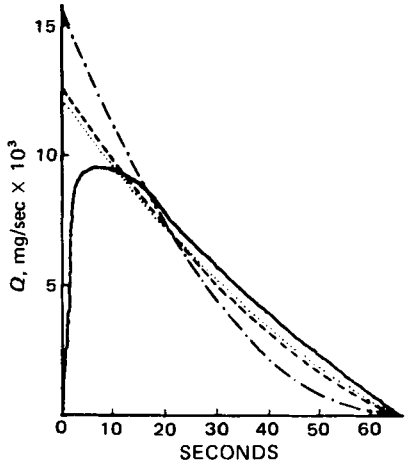

Figure 11—*Comparison of the ability of Eqs. 11, 22, and 23 to describe the dissolution of Crystal 1 (Tables II and III). Key: —, experimental line; ···, Eq. 22; -·-·, Eq. 11; and ---, Eq. 23.*

Two different cases can be identified:

1. The calculated value of b is about the same as the measured value for b_0. The ratios d/b_0 and d/l_0 then are roughly 1/2 (Crystal 1, Tables II and III), as is the ratio of the particle obeying the cube root law, so the effect of shape is minimal. Therefore, Eq. 23 describes the dissolution process almost as accurately as Eq. 22. The difference between Eqs. 11 and 23 is significant (Fig. 11). This difference is caused only by the slower and nonlinear dissolution rate of crystal face J.

2. Especially when b is smaller than b_0, a large deviation can be expected due to the combined effects of shape and the retreat rate of face J. A representative crystal of this class is Crystal 2 (Tables II and III). Since the lifetime of a crystal of potassium ferricyanide is determined by b_0, the slower and nonlinear dissolution rate of face J has no influence on crystal lifetime. Therefore, the deviation in prediction of $t = T$ (ΔT, Table II) is the same for Eqs. 11 and 23 and illustrates purely the effect of shape, which can be quite substantial (up to 25% for these crystals).

Results of this investigation can be summarized as follows. The close agreement between the measured curve and the one calculated with Eq. 22 usually justifies the use of a constant and equal retreat rate for all crystal faces except one. If there is a relative motion between a dissolving crystal and the solvent, there is always a face at the rear side of the crystal at which the flow pattern is different. This situation makes it necessary to use a lower value for this face for the retreat rate, which, according to the present measurements, increases as dissolution proceeds. This effect has a bearing on nonisometric as well as isometric particles.

Furthermore, the effect of shape is important. An apparent increase in the rate constant will be measured if isometric dissolution behavior is postulated for particles that have the shortest diameter terminating the dissolution process.

REFERENCES

(1) A. W. Hixson and J. H. Crowell, *Ind. Eng. Chem.*, **23**, 923 (1931).

(2) P. J. Niebergall, G. Milosovich, and J. E. Goyan, *J. Pharm. Sci.*, **52**, 236 (1963).

(3) A. W. Hixson and J. H. Crowell, *Ind. Eng. Chem.*, **23**, 1160 (1931).

(4) R. H. Wilhelm, L. H. Conklin, and T. C. Sauer, *ibid.*, **33**, 453 (1941).

(5) W. L. McCabe and R. P. Stevens, *Chem. Eng. Proc.*, **47**, 168 (1951).

(6) P. Veng Pederson and H. F. Brown, *J. Pharm. Sci.*, **65**, 1437 (1976).

(7) *Ibid.*, **65**, 1442 (1976).

ACKNOWLEDGMENTS

The authors thank F. Stuurman and P. Plouvier for their valuable contribution to the design of the continuous-flow recording apparatus.